

## Original Research

# Molecular subtype classification of breast cancer using established radiomic signature models based on $^{18}\text{F}$ -FDG PET/CT images

Jianjing Liu<sup>1,†</sup>, Haiman Bian<sup>2,†</sup>, Yufan Zhang<sup>1,3,†</sup>, Yongchang Gao<sup>4</sup>, Guotao Yin<sup>1</sup>, Ziyang Wang<sup>1</sup>, Xiaofeng Li<sup>1,\*</sup>, Wenjuan Ma<sup>5,\*</sup>, Wengui Xu<sup>1,\*</sup>

<sup>1</sup>Department of Molecular Imaging and Nuclear Medicine, Tianjin Medical University Cancer Institute and Hospital, National Clinical Research Center for Cancer, Key Laboratory of Cancer Prevention and Therapy, Tianjin's Clinical Research Center for Cancer, 300060 Tianjin, China, <sup>2</sup>Department of Radiology, Tianjin Medical University Cancer Institute and Hospital, National Clinical Research Center for Cancer, Key Laboratory of Cancer Prevention and Therapy, Tianjin's Clinical Research Center for Cancer, 300060 Tianjin, China, <sup>3</sup>Department of Nuclear Medicine, Southwest Hospital, The First Affiliated Hospital to Army Medical University, 400038 Chongqing, China, <sup>4</sup>Department of General Surgery, Tianjin Medical University General Hospital, 300060 Tianjin, China, <sup>5</sup>Department of Breast Imaging, Tianjin Medical University Cancer Institute and Hospital, National Clinical Research Center for Cancer, Key Laboratory of Cancer Prevention and Therapy, Tianjin's Clinical Research Center for Cancer, 300060 Tianjin, China

## TABLE OF CONTENTS

1. Abstract
2. Introduction
3. Materials and methods
  - 3.1 Patient characteristics
  - 3.2  $^{18}\text{F}$ -FDG PET/CT imaging
  - 3.3 Molecular subtype classification
  - 3.4 Extraction and measurement of radiomic features based on PET/CT images
  - 3.5 Statistical analyses
4. Results
  - 4.1 The workflow of the present investigation
  - 4.2 Comparison of conventional PET parameters between different groups of BC patients based on molecular subtype classification
  - 4.3 Predictive power of PET/CT-derived multivariate radiomic signature models for molecular subtype classification of BC
  - 4.4 The mean performances of the established radiomic signature models in discriminating molecular subtypes of BC
5. Discussion
6. Conclusions
7. Author contributions
8. Ethics approval and consent to participate
9. Acknowledgment
10. Funding
11. Conflict of interest
12. References

## 1. Abstract

**Backgrounds:** To evaluate the predictive power of  $^{18}\text{F}$ -Fluorodeoxyglucose positron emission tomography/computed tomography ( $^{18}\text{F}$ -FDG PET/CT) derived radiomics in molecular subtype classification of breast cancer (BC). **Methods:** A total of 273 primary BC patients

who underwent a  $^{18}\text{F}$ -FDG PET/CT imaging prior to any treatment were included in this retrospective study, and the values of five conventional PET parameters were calculated, including the maximum standardized uptake value (SUVmax), SUVmean, SUVpeak, metabolic tumor volume (MTV), and total lesion glycolysis (TLG). The ImageJ 1.50i

software and METLAB package were used to delineate the contour of BC lesions and extract PET/CT derived radiomic features reflecting heterogeneity. Then, the least absolute shrinkage and selection operator (LASSO) algorithm was used to select optimal subsets of radiomic features and establish several corresponding radiomic signature models. The predictive powers of individual PET parameters and developed PET/CT derived radiomic signature models in molecular subtype classification of BC were evaluated by using receiver operating curves (ROCs) analyses with areas under the curve (AUCs) as the main outcomes. **Results:** All of the three SUV parameters but not MTV nor TLG were found to be significantly underrepresented in luminal and non-triple (TN) subgroups in comparison with corresponding non-luminal and TN subgroups. Whereas, no significant differences existed in all the five conventional PET parameters between human epidermal growth factor receptor 2+ (HER2+) and HER2- subgroups. Furthermore, all of the developed radiomic signature models correspondingly exhibited much more better performances than all the individual PET parameters in molecular subtype classification of BC, including luminal vs. non-luminal, HER2+ vs. HER2-, and TN vs. non-TN classification, with a mean value of 0.856, 0.818, and 0.888 for AUC. **Conclusions:** PET/CT derived radiomic signature models outperformed individual significant PET parameters in molecular subtype classification of BC.

## 2. Introduction

As reported in cancer statistics in 2019, breast cancer (BC) is one of the most common malignancies in women worldwide, ranking first in prevalence and second in mortality [1]. Histological type and grade, proliferative activity and status of human epidermal growth factor receptor 2 (HER2) and hormone receptors expression are increasingly accepted as the most common characteristics influencing the choice of treatment options, the evaluation of therapy responses and the prediction of survival for patients with BC [2, 3]. Consistently, BC is categorized into four different molecular subtypes based on expression of hormonal receptors and HER2 status, including Luminal subtype: hormone receptor positive, HER2 negative; Luminal/HER2 positive subtype: hormone receptor positive, HER2 overexpression or amplified; HER2 positive non-luminal subtype: hormone receptor negative, HER2 overexpression or amplified; Triple-negative (TN) subtype: hormone receptor negative and HER2 negative [4]. However, this molecular subtype classification is mainly achieved through invasive procedures, such as biopsy-based immunohistochemical (IHC) staining or fluorescence in situ hybridization (FISH) method [5]. Moreover, heterogeneity existed in different BC lesions from individual BC patients, even in a same lesion from a single BC patient [6]. Therefore, the local biopsy could not represent the whole tumor lesion or the distant unexamined metastatic lesions due to the existed

heterogeneity in BC lesions. A reliable and non-invasive imaging methodology is needed to identify these gene expression profiles to develop personalized treatment and improve early prognosis prediction for patients with BC [7–10].

As a hybrid imaging allowing for simultaneous anatomic imaging and molecular functional imaging,  $^{18}\text{F}$ -Fluorodeoxyglucose positron emission tomography/computed tomography ( $^{18}\text{F}$ -FDG PET/CT) imaging is already widely used in tumor detection, tumor staging, treatment response evaluation and survival prediction based on the provided functional information about tumor glucose metabolism for a variety of tumors, including BC [11]. Standardized uptake value (SUV), metabolic tumor volume (MTV) and total lesion glycolysis (TLG) are most commonly used semi-quantitative parameters extracted from PET images [12]. Furthermore, these traditional PET parameters have been found to be correlated to hormone receptors status and molecularly defined subtypes for patients with BC [13, 14]. Nevertheless, especially for SUV as a single pixel value, it is not able to adequately reflect the glucose metabolism of the whole tumor with heterogeneity [15].

It is now recognized that standard medical images may contain more useful information than that we can see by using our naked eyes. Radiomics is an emerging hot topic in medical imaging, which is actually a high-throughput extraction of quantitative metrics from medical images via computational post-processing techniques [4, 9, 10]. Indeed, radiomics is based on the assumption that the extracted heterogeneity descriptors from medical images are linked to genotypic and molecular characteristics of the tumor lesions, and is believed to be a promising model to guide patient management in personalized medicine [16]. To date, most studies about radiomics in relation to molecular characterization of BC are ultrasound [7], mammographic [17] and magnetic resonance imaging (MRI) radiomics [9, 10, 18–20]. Few data regarding to PET/CT radiomics for BC patients are available, especially for the performance of radiomics models based on PET/CT images in molecular subtype determination [4, 21, 22].

In the present investigation, the heterogeneity in  $^{18}\text{F}$ -FDG PET/CT images of primary BC lesions was quantitatively measured by radiomic analyses and several multi-feature radiomic signature models were developed to evaluate the predictive performance of radiomics based on PET/CT images in molecular subtype determination for patients with BC.

## 3. Materials and methods

### 3.1 Patient characteristics

In this retrospective single center investigation, the following specific inclusion/exclusion criteria were applied to select eligible patients from Tianjin Medical Uni-

versity Cancer Institute and Hospital between 1st January 2010 and 31st May 2019: (1) age  $\geq 18$  years; (2) good mammary condition evaluated by clinical tests, mammography and mammary ultrasonography within 3 months prior to  $^{18}\text{F}$ -FDG PET/CT imaging; (3)  $^{18}\text{F}$ -FDG PET/CT imaging performed at our institution before any treatment; (4) histological diagnosis of primary BC at any clinical stage using pathological examination of mammary biopsy or surgical histological specimen. Patients with pregnancy, breast feeding and any previous relevant treatment were excluded from this study. A total of 273 patients were included in this study (age  $51.76 \pm 10.81$ , range, 26–78 years). General clinical data were collected from all the included participants, and all the clinicopathological characteristics collected were summarized in Table 1. This retrospective study was reviewed and approved by our institutional ethics committee and conducted in compliance with the Declaration of Helsinki and relevant ethical guidelines. Written informed consent was waived from all included patients in this study.

### 3.2 $^{18}\text{F}$ -FDG PET/CT imaging

After at least 6 h of fasting, BC patients with blood glucose levels less than 140 mg/dL received an intravenous injection of 4 MBq/kg of  $^{18}\text{F}$ -FDG. Then a whole body  $^{18}\text{F}$ -FDG PET/CT imaging on a GE Discovery elite (GE HealthCare, Chicago, IL, USA) was performed 1 hour after the planned intravenous administration of  $^{18}\text{F}$ -FDG. A low-dose helical CT (helical pitch 0.75 : 1, 5 mm slice thickness, 120 kV and 50–80 mAs) was first performed for anatomical correlation and attenuation correction, followed by a PET emission scan of 2 min per bed position in a three-dimensional mode. The CT-based attenuation-corrected PET images were reconstructed using an iterative algorithm. All PET images were then converted in SUV units using standardization by the injection dose and subject's body weight. The volume of interest (VOI) was determined using an isocontour threshold method based on SUV, which was delineated using a 42% threshold of the maximum SUV (SUV<sub>max</sub>). Then, SUV<sub>max</sub>, SUV<sub>mean</sub> and SUV<sub>peak</sub> were calculated automatically within the VOI to determine the intensity of FDG uptake semi-quantitatively using a commercial software (PET VCAR, GE Healthcare, Waukesha, WI, USA) on a GE Advantage Workstation 4.6 (AW 4.6). All primary BC lesions included showed metabolic  $^{18}\text{F}$ -FDG uptake (SUV<sub>max</sub>  $\geq 2.5$ ). MTV was defined as a volumetric measurement of lesion with significantly high  $^{18}\text{F}$ -FDG uptake above a threshold SUV of 2.5. Whereas, TLG represents another volumetric index, which is achieved by multiplying MTV by SUV<sub>mean</sub>. All PET images reconstruction, VOI delineation, index calculation were reviewed in consensus by two experienced PET/CT imaging-specialized experts.

**Table 1. Patients' characteristics (n = 273).**

Characteristics	n (%)
Sex	
Female	273 (100%)
Male	0 (0%)
Age	51.76 $\pm$ 10.81
Histology	
Invasive ductal carcinoma	263 (96.34%)
Invasive lobular carcinoma	3 (1.10%)
Others	7 (2.56%)
ER	
Positive	181 (66.30%)
Negative	92 (33.70%)
PR	
Positive	156 (57.14%)
Negative	117 (42.86%)
HER2	
Positive	106 (38.83%)
Negative	167 (61.17%)
Ki-67	
<20%	34 (12.45%)
$\geq 20\%$	239 (87.55%)
N staging	
Positive	222 (81.32%)
Negative	51 (18.68%)
M staging	
Positive	55 (20.14%)
Negative	218 (79.86%)
Staging	
I	19 (6.96%)
II	139 (50.92%)
III	60 (21.98%)
IV	55 (20.14%)
Subtype	
Luminal A	20 (7.33%)
Luminal B (HER2-)	106 (38.83%)
Luminal B (HER2+)	61 (22.34%)
HER2 Subtype	45 (16.48%)
Triple Negative	41 (15.02%)

ER, estrogen receptor; HER2, human epidermal growth factor receptor 2; n, number; N, node; M, metastasis; PR, progesterone receptor.

### 3.3 Molecular subtype classification

Molecular subtype classification of patients with BC in this study was based on the status of hormone receptors and HER2 expression as mentioned previously. Briefly, patients with positive immunohistochemical (IHC) expression of estrogen receptor (ER) and progesterone receptor (PR) regardless of the status of HER2 were defined as Luminal subtype; patients with overexpression or amplification of HER2 regardless of the status of ER or PR were divided into HER2 positive (HER2+) subtype; patients with negative IHC expression of hormone receptors and negative amplification of HER2 were determined as triple negative

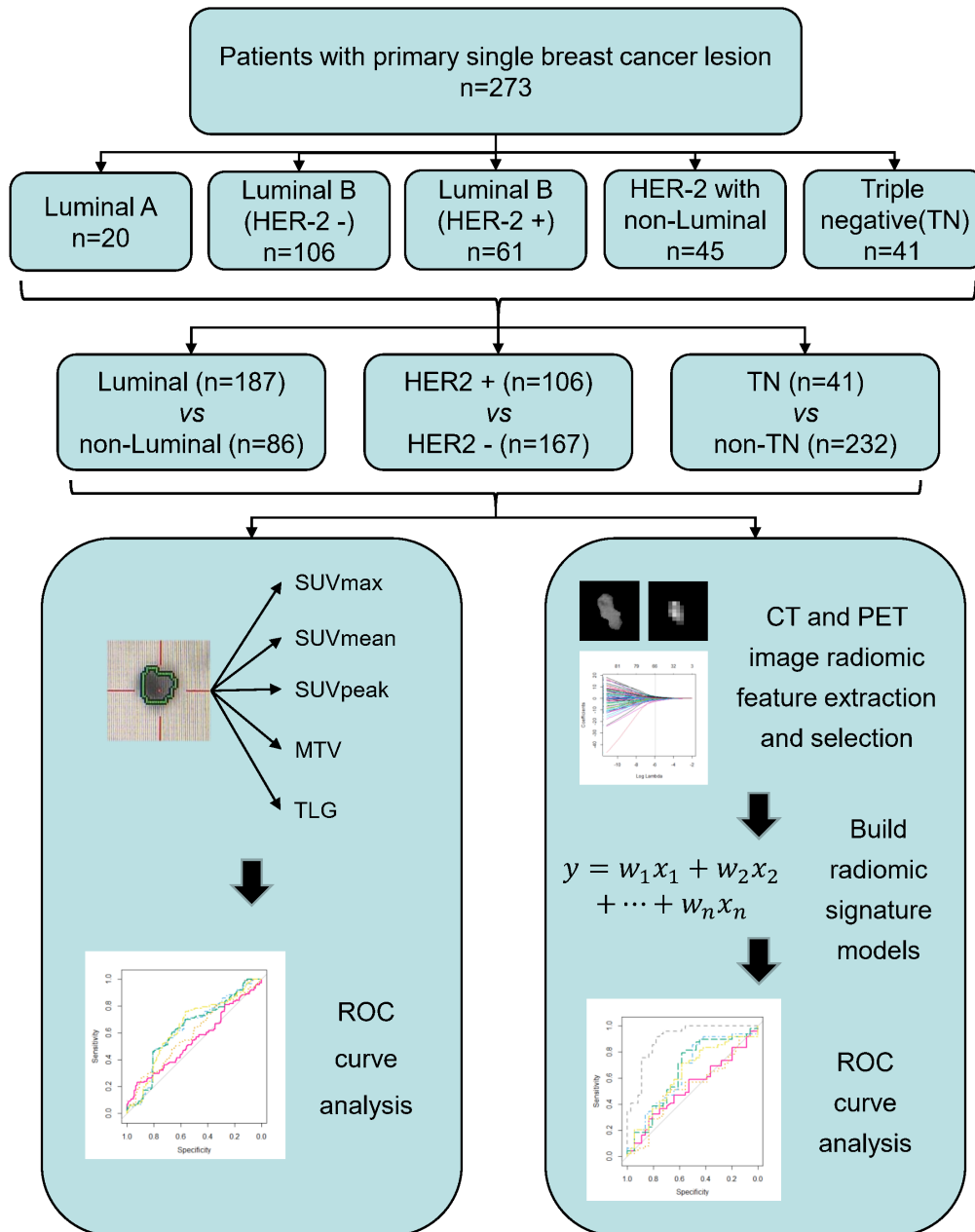


**Fig. 1. The workflow of this study.** Briefly, a total of 273 eligible BC patients were enrolled in the radiomic analysis. Based on the molecular subtypes classification by IHC or FISH assay, BC patients were divided into different groups for comparison, including Luminal vs. Non-luminal, HER2+ vs. HER2- and TN vs. Non-TN. Radiomic analysis in the study mainly consist of lesion segmentation, radiomic features extraction and selection, multivariate radiomic signature model construction, and evaluation of the predictive performance of the developed radiomic signature model in molecular subtypes classification of BC by ROC analysis. Apart from radiomic analysis, a total of 5 conventional PET parameters (SUVmax, SUVmean, SUVpeak, MTV and TLG) were also calculated to compare their abilities to discriminate between different molecular subtypes of BC with that of established radiomic signature model.

BC, breast cancer; CT, computed tomography; FISH, fluorescence in situ hybridization; HER2, human epidermal growth factor receptor 2; IHC, immunohistochemistry; MTV, metabolic tumor volume; PET, positron emission tomography; ROC, receiver operating curve; SUV, standardized uptake value; TLG, total lesion glycolysis; TN, non-triple.

(TN) subtype. It was important to note that the status of HER2 were assessed by both IHC staining and FISH assay. Especially for patients with ambiguous results of IHC staining of HER2, FISH was used to finally determine the status of HER2.

### 3.4 Extraction and measurement of radiomic features based on PET/CT images

To extract radiomic features from PET/CT images, the contour of the region of interest (ROI) on PET or CT images was firstly manually outlined by two ex-

perienced PET/CT imaging-specialized experts using ImageJ 1.50i software (National Institute of Health, Bethesda, MD, USA). Any disagreement about the delineation was resolved by consensus. Then, over the segmented tumor ROI, all radiomic features were calculated by applying an existing automated computer program (MATLAB, The MathWorks Inc., Natick, MA, USA). A total of 1710 quantitative radiomic features (855 PET-based and 855 CT-based radiomic features) were extracted and calculated from PET/CT images. Data augmentation was used to smooth the imbalance between groups. To assess their performances in molecular subtype determination of patients with BC, including Luminal vs. Non-Luminal, HER2 positive (HER2+) vs. HER2 negative (HER2-) and TN vs. Non-TN, multivariate radiomic signature models based on PET/CT radiomic features were developed in the present investigation.

### 3.5 Statistical analyses

For quantitative variables, results were expressed as mean  $\pm$  standard deviation, whereas for categorical variables, numbers and percentages were used. Wilcoxon rank-sum test was used to determine the difference existed in each conventional PET parameters between BC patients groups with different molecular subtypes. Multivariate radiomic signature models were developed by following a three-step procedure to identify robust radiomic features. First, wilcoxon test was used to select features that were highly related to the biomarkers. A significance level of 0.05 ( $p < 0.05$ ) was set as the threshold. An interfeature coefficient (R) between all possible pairs of features was subsequently used to eliminate high-dimensional feature redundancy.  $R > 0.80$  was the cutoff for strong relationships, in which 1 of 2 features with a lower  $p$  value was excluded. Next, the least absolute shrinkage and selection operator (LASSO) cox regression method was used to select the most predictive features. Then, the radiomics score (Rad-score) was computed for each patient through a linear combination of selected features weighted by their respective coefficients. The area under curve (AUC) in receiver-operating-characteristic (ROC) curve analysis was used to evaluate the performance of individual PET parameter, established radiomic signature models in molecular subtype classification of patients with BC. Finally, a 10-fold cross validation with 10 times repetition was used to calculate the average performance of these developed radiomic signature models in consideration of the relatively small sample size in this study. Analyses were performed using R statistical software (version 3.2.2, The R Foundation for Statistical Computing, Vienna, Austria), and difference with a  $p$ -value less than 0.05 was interpreted as statistically significant.

## 4. Results

### 4.1 The workflow of the present investigation

To evaluate the predictive power of  $^{18}\text{F}$ -FDG PET/CT derived radiomics in molecular subtype classification of BC, a total of 273 BC patients who underwent  $^{18}\text{F}$ -FDG PET/CT imaging prior to any treatment were included in the study. The different group division of BC patient, including Luminal vs. Non-Luminal, HER2 positive (HER2+) vs. HER2 negative (HER2-) and TN vs. Non-TN, was based on the status of ER, PR and HER2 expression by IHC assay or FISH assay. First, conventional PET parameters, including SUVmax, SUVmean, SUVpeak, MTV and TLG, were calculated and compared between different groups. Then, radiomic features based on PET/CT images were extracted and selected to develop multivariate radiomic signature models in the study, and the predictive power of these established PET/CT-derived multivariate radiomic signature models for molecular subtype classification of BC was evaluated by ROC analyses. The workflow of the study was charted in Fig. 1.

### 4.2 Comparison of conventional PET parameters between different groups of BC patients based on molecular subtype classification

Of the 273 BC patients with results for molecular subtype classification, 68.5% (187/273) of patients were defined as Luminal subtype and 38.8% (106/273) of patients were with a HER2 positive regardless of hormone receptors status (HER2+), whereas 15.0% (41/273) of patients were tested negatively for both hormone receptors and HER2, known as TN subtype. To assess the association between conventional PET parameters (SUVmax, SUVmean, SUVpeak, MTV and TLG) and molecular subtype classification, we first compared the conventional PET parameter values between groups with different molecular profiles (Table 2). For Luminal BC patients, the SUVmax, SUVmean and SUVpeak were found to be underrepresented in comparison with the Non-Luminal group, whereas no significant difference of MTV or TLG existed between Luminal vs. Non-Luminal. With respect to HER2+ vs. HER2-, no significant differences existed between HER2+ BC patients and HER2- patients for all the five conventional PET parameters. As expected, the TN subtype group demonstrated significantly higher values of SUVmax, SUVmean and SUVpeak, but not for MTV or TLG in contrast with Non-TN subtype BC patients.

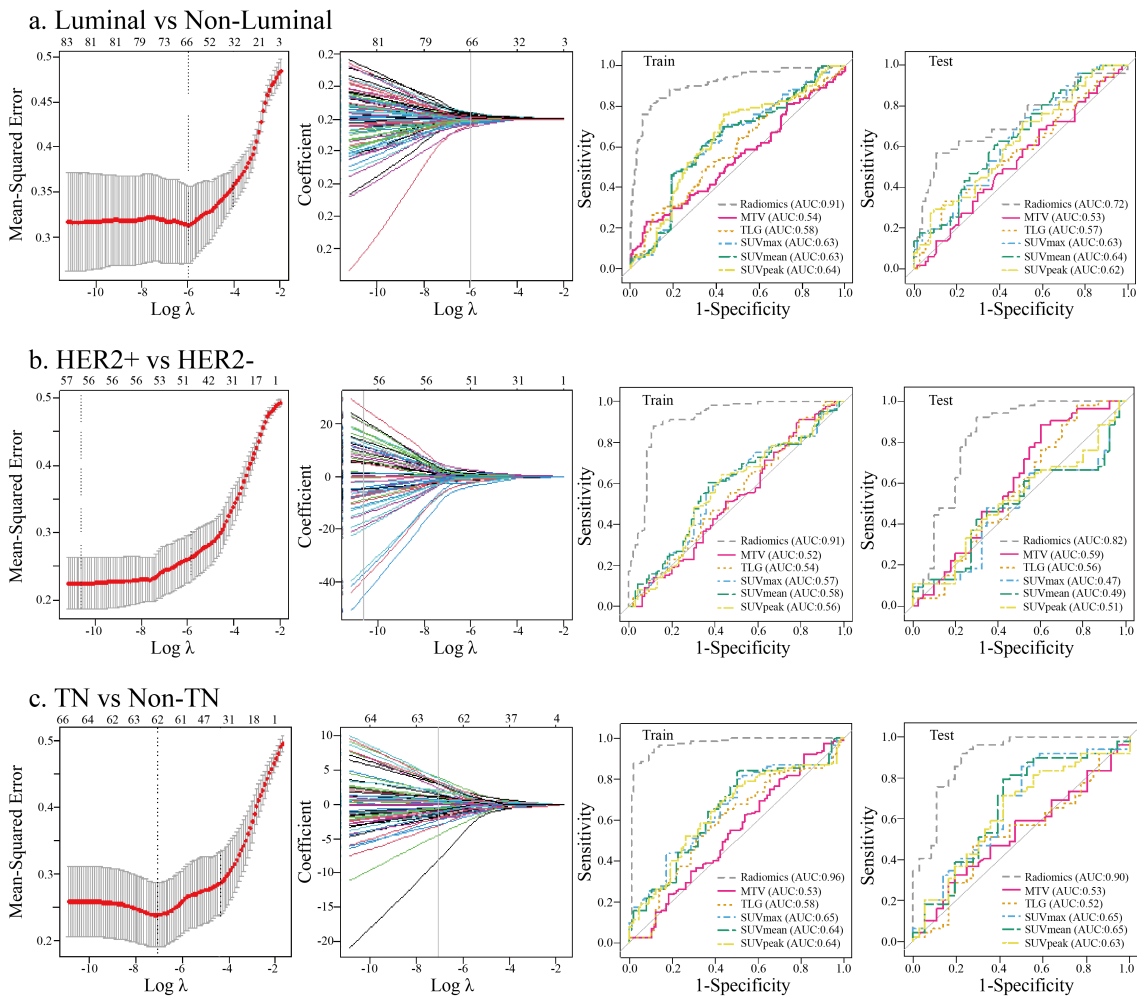
### 4.3 Predictive power of PET/CT-derived multivariate radiomic signature models for molecular subtype classification of BC

A total of 1710 radiomic features (855 PET-based and 855 CT-based radiomic features) were extracted and computed based on PET/CT images. After LASSO regression (Fig. 2), the most predictive radiomic features based on PET/CT images were selected to establish radiomic signa-

**Table 2. Comparison of conventional PET parameters based on molecular subtype classification of breast cancer.**

	<i>n</i>	SUVmax	SUVmean	SUVpeak	MTV	TLG
Luminal	187	9.29 ± 5.50	5.72 ± 3.42	6.93 ± 4.68	16.40 ± 33.67	142.36 ± 339.75
Non-Luminal	86	12.21 ± 6.67	7.49 ± 3.99	9.02 ± 5.48	23.75 ± 101.11	239.38 ± 987.40
<i>p</i>		<0.001	<0.001	0.001	0.993	0.173
HER2+	106	10.65 ± 5.67	6.59 ± 3.45	7.88 ± 4.54	14.53 ± 30.69	143.06 ± 359.39
HER2-	167	9.94 ± 6.31	6.08 ± 3.84	7.40 ± 5.32	21.37 ± 76.88	191.89 ± 741.13
<i>p</i>		0.132	0.113	0.121	0.509	0.949
TN	41	12.70 ± 9.36	7.68 ± 4.27	9.44 ± 6.17	33.86 ± 144.49	316.61 ± 1378.81
Non-TN	232	9.78 ± 5.68	6.03 ± 3.54	7.26 ± 4.74	16.04 ± 32.02	147.53 ± 347.25
<i>p</i>		0.015	0.019	0.031	0.566	0.567

HER2, human epidermal growth factor receptor 2; MTV, metabolic tumor volume; *n*, number; PET, positron emission tomography; SUV, standardized uptake value; TLG, total lesion glycolysis; TN, non-triple.

**Fig. 2. The predictive power of established PET/CT derived multivariate radiomic signature models in molecular subtypes classification of BC.**

The LASSO algorithm and 10-fold cross-validation were used to extract the optimal subsets of PET/CT derived radiomic features for molecular subtypes classification of BC, including Luminal vs. Non-luminal (a), HER2+ vs. HER2- (b), TN vs. Non-TN (c). In the first column, the dash lines represented the optimal  $\lambda$  selected by 10-fold cross validation, which have the minimum mean square error (red dots). The second column showed LASSO coefficient profiles of the selected subsets of radiomic features at the optimal  $\lambda$  (grey line) for molecular subtypes classification of BC. The third and fourth columns showed the ROC curves of the established multivariate radiomic signature models for molecular subtypes classification of BC in comparison with that of each conventional PET parameters in both the training and the validation cohorts. For each molecular molecular subtype classification, the performance of the radiomic signature model outperformed all the conventional PET parameters.

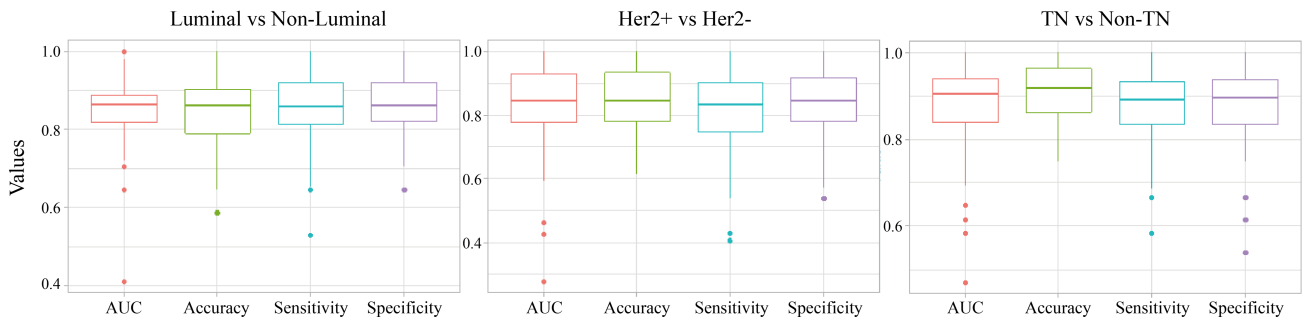


**Fig. 3. The distribution of AUC, accuracy, sensitivity and specificity of the established radiomic signature models in molecular subtypes classification of BC in the 10-fold cross validation.** The thick lines represent the median of performance indicators. The median AUC, accuracy, sensitivity and specificity were used to describe the predictive power of each established radiomic models in each molecular subtype classification of BC, including including Luminal vs. Non-Luminal (left), HER2 + vs. HER2 - (middle), TN vs. Non-TN (right).

ture models for molecular subtype classification of BC. As presented in **Supplementary Fig. 1**, three most predictive sets of radiomic features were included in each established multivariate radiomic signature models, including Luminal vs. Non-Luminal (**Supplementary Fig. 1A**), HER+ vs. HER2- (**Supplementary Fig. 1B**) and TN vs. Non-TN (**Supplementary Fig. 1C**). In addition, the formulas to compute the radiomics score (Rad-score) for each patient through a linear combination of selected features weighted by their respective coefficients in each established multivariate radiomic signature models were also listed in the **Supplementary materials**. To evaluate the performance of established radiomic signature models in distinguishing molecular subtypes of BC, ROC analyses were conducted and AUCs were used as the main outcomes. As shown in Fig. 2, all the three established multivariate radiomic signature models significantly outperformed all the conventional PET parameters (SUVmax, SUVmean, SUVpeak, MTV and TLG) in molecular subtype classification of BC, with a AUC of 0.913 and 0.725, 0.912 and 0.820, 0.968 and 0.901 for Luminal vs. non-Luminal (Fig. 2a), HER+ vs. HER2- (Fig. 2b) and TN vs. non-TN (Fig. 2c) discrimination in the training set and the validation set, respectively. In consideration of a significant association between SUV parameters and molecular subtype classification of BC, several integrated models by taking into account not only PET/CT derived radiomic features but also SUV parameters were established to assess their performance in molecular subtype classification of BC. A comparable but not a superior performance of integrated models in molecular subtype classification compared to radiomic signature models was observed.

#### 4.4 The mean performances of the established radiomic signature models in discriminating molecular subtypes of BC

In consideration of the aforementioned relatively small sample size in this investigation, a 10-fold cross validation with 10 times repetition was used to calculate the average performance of each of these three established ra-

diomic signature models in each molecular subtypes classification, including Luminal vs. Non-Luminal, HER+ vs. HER2- and TN vs. Non-TN. As demonstrated in Fig. 3, each of these three developed radiomic signature models based on PET/CT images correspondingly exhibited a strong predictive power in each molecular subtype classification of BC, with a mean value of 0.856, 0.818 and 0.888 for AUC, a mean value of 0.864, 0.847 and 0.893 for accuracy, a mean value of 0.801, 0.908 and 0.933 for sensitivity and a mean value of 0.905, 0.764 and 0.839 for specificity. These results described above significantly suggest the stability of the outperformance of established radiomic signature models in molecular subtype classification of BC.

## 5. Discussion

Results with respect to correlation between molecular subtypes of BC and imaging-derived parameters had been published previously [12–15]. Especially, texture feature quantification and analyses based on medical images are of increasing interest to a large number of investigators addressing the interaction between quantitative imaging radiomic features and tumor molecular profiling [4, 16]. Moreover, considering breast cancer is a heterogeneous class of tumor, radiomic analyses aiming at elucidating the tumor heterogeneity reflected in medical images would enable an accurate prediction of tumor biological characteristics and genetic profiling. The primary objective of this current study was to evaluate the potential of  $^{18}\text{F}$ -FDG PET/CT derived radiomic signature models to distinguish between different molecular subtypes of BC, because of the unique advantage of  $^{18}\text{F}$ -FDG PET/CT imaging over other imaging modalities, such as mammography [17], ultrasound [7] and MRI [9]. As shown, BC lesions with luminal subtype exhibited significantly lower FDG radioactivity uptake (SUVmax, SUVmean and SUVpeak) compared to that with non-luminal subtype. Similarly, all of the three SUV parameters were found to be markedly underrepresented in BC patients with non-TN subtype in con-

trast with BC patients with TN subtype. Whereas, no substantial association was demonstrated between HER2+ BC patients and HER2- BC patients for all the five conventional PET parameters. These results demonstrated that different molecular subtypes of BC underlined the differences described in FDG uptake by BC lesions *in vivo*, which is increasingly recognized because it was previously reported that BC lesions with an aggressive subtype, such as non-luminal or TN, tended to be with an increase in glucose metabolism which could be captured and reflected in SUV parameters (SUVmax, SUVmean and SUVpeak) [13–15]. Whereas, PET volumetric parameters, such as MTV and TLG, which are always used to represent the tumor burden, were found to be not significantly different between different BC subgroups with different molecular subtypes. With regard to the discrimination between HER2+ and HER2- subgroups by conventional PET parameters, because both lower-glucose-metabolic BC with luminal subtype and higher-glucose-metabolic BC with TN were categorized into HER2- subgroup, which would lead to the negative results about HER2+ vs. HER2- classification by using conventional PET parameters.

Expectedly, established multivariate radiomic signature models as shown in **Supplementary Fig. 1** remarkably outperformed all the significant SUV parameters in discrimination between different molecular subtypes of BC. In comparison with previous literature with regard to the association between radiomic features based on PET images alone and molecular subtypes of BC [4, 21, 22], our current investigation had a larger sample size and performed a comprehensive radiomic analysis involving both PET-based and CT based radiomic features. Particularly in contrast with results from ZY Yang *et al.* [21], which only focused on the discrimination between ER+ and ER-, our study consist of analysis with regard to Luminal vs. Non-Luminal, HER2+ vs. HER2- and TN vs. non-TN. In this context, the results listed in our investigation would provide an essentially complementary information about PET/CT derived radiomic analyses in molecular characterization of BC. Moreover, because selecting individual radiographic parameters which were not remarkably correlated to each other could provide added information but not overlapping messages with respect to various aspects of tumor lesion heterogeneity, multivariate radiomic signature model as presented in **Supplementary Fig. 1** but not individual radiomic feature was used in our study to directly evaluate the performance of PET/CT derived radiomics in molecular subtype classification of BC, which was lacking in previous relevant investigations. To some extent, molecular subtype classification is a brilliant method to reflect the heterogeneity in BC and is helpful for personalized medicine of BC patients [2, 3]. For BC patients with HER2 enrichment, a sophisticated intracellular signaling initiated by HER2 activation on the membrane of breast cancer cells leads to an enhanced metabolism and a subsequently ag-

gressive behavior of HER2-enriched breast cancer in contrast with breast cancer without HER2 accumulation [23]. Considering the tumor-promoting action of HER2 in breast cancer, targeted therapies against HER2 were developed and applied to clinical management, namely trastuzumab (Trade name: Herceptin) treatment [24]. To improve the performance of HER2-targeted therapy for BC in clinic and make a dramatic progress in precision medicine, a precise assessment of the target HER2 prior to treatment is essential. As known, HER2 status was most commonly tested via IHC examination, and cases with ambiguous results usually refer to FISH assay. A subgroup radiomic analysis focusing on a cohort of BC patients who underwent a FISH assay to finally identify HER2 status because of their equivocal IHC results of HER2 status is planed in our future study. The abilities of PET/CT derived radiomic signature models to discriminate molecular subtypes of BC suggest an underlined molecular profile-involving mechanism for heterogeneity reflected by PET/CT derived radiomic features [6]. Even though BC patients could benefit from current molecular subtype classification to guide their clinical management, such as treatment options, outcome prediction and survival prognosis, more and more investigation have discovered heterogeneity existed in the same molecular subtype of BC within individuals and between individuals. The existed heterogeneity in sensitivities to some targeted therapies and neoadjuvant treatment for BC patients with the same molecular subtype and the development of acquired treatment resistance prompt us to further determine the performance of radiomic signature model based on PET/CT images in these concerning issues, which is what we strive to do in near future.

The ultimate goal of accurate molecular subtype classification for BC patients is to individualise therapy and achieve precision medicine. Multidisciplinary therapeutic approaches, including hormone therapy, HER2-targeted therapy, chemotherapy and radiotherapy are precisely chosen for BC patients based on molecular profile determination. Radiomics and artificial intelligence development have not only shed light on molecular subtype profiling, but also for other various aspect of clinical practice for BC patients, such as diagnosis, treatment response prediction and survival prognosis [25]. Especially for neoadjuvant radiotherapy or chemoradiotherapy, radiomics and artificial intelligence have exhibited a potential for clinical translation in tailed treatment prediction [26–28]. With respect to BC patients, radiological image derived artificial intelligence-based decision supporting system for radiotherapy would be beneficial to patient consultation, target volume delineation, automated treatment planning, treatment delivery and response evaluation and prediction [29]. Furthermore, an enhanced prediction of neoadjuvant chemoradiotherapy response by using PET/CT radiomic models with an addition of HER2 information suggested that accurate HER2 status determination based on radiomics would be remark-

ably helpful to comprehensive treatment strategy involving radiotherapy and targeted therapy [28].

Despite those encouraging results depicted in this study, several limitations existed in this current work. First, given the relatively small sample size in this radiomic analysis, further investigation involving a larger number of cases is warranted to confirm the results obtained in the study. Second, the varieties in acquisition, reconstruction and delineation settings maybe affect the repeatability of radiomic analyses due to the retrospective nature of this study. A prospective, multicenter research with a standardization and optimization for these settings is needed to overcome these drawbacks. Then, a relatively limited spatial resolution of PET may result in an unsatisfactory performance of PET related radiomics in breast cancer, in particular for patients with small lesion. In addition, this study only focused on primary breast cancer lesions but not on metastatic lesions, therefore a further investigation involving both primary and metastatic lesions is required to complete this study [30]. Last but not least, to comprehensively determine the phenotype-genotype interaction, radiomic analyses based on not only a binary-classification but also on a multi-classification for molecular subtype clustering of BC should be included, which is exactly what we aim to do in future.

## 6. Conclusions

Taken together, distinct imaging phenotypes driven by different molecular profiling of BC may be captured in  $^{18}\text{F}$ -FDG PET/CT images and quantitatively measured by radiomic features. Established multivariate radiomic signature models based on  $^{18}\text{F}$ -FDG PET/CT images could provide more information than conventional individual PET parameters which are currently widely used for clinical imaging, enabling a precise reflection of tumor heterogeneity.

## 7. Author contributions

JL, HB and YZ contributed equally and are co-first authors; JL and HB designed experiments; JL, HB and YZ performed experiments; JL, HB, YZ and XL wrote the manuscript; GY, YG and ZW analyzed data; YG synthesized and interpreted the results. XL, WM and WX supervised the study and made manuscript revisions. All authors gave final approval of the version to be published and have agreed on the submitted journal. And all authors agreed to be accountable for all aspects of the work.

## 8. Ethics approval and consent to participate

All procedures performed in studies involving human participants were in accordance with the declaration of Helsinki and relevant approved guidelines and approved by the Ethical Review Committee of Tianjin Medical Univer-

sity Cancer Institute and Hospital, and the ethical approval code is Ek2018125. Written informed consent from all patients was waived in the present investigation.

## 9. Acknowledgment

We would like to thank all the study participants, research staff, and students who participated in this work. In addition, we are really appreciated for the invaluable comments on this study from all the reviewers.

## 10. Funding

This work was supported by grants from the National Natural Science Foundation of China (grant nos. 81801781, 82072004, 2018ZX09201015), the Tianjin Science and Technology Committee Fund (grant nos. 18PTZWHZ00100 and H2018206600), the Science & Technology Development Fund of Tianjin Education Commission for Higher Education (grant nos. 2018KJ057 and 2018KJ061).

## 11. Conflict of interest

The authors declare no conflict of interest.

## 12. References

- [1] Siegel RL, Miller KD, Jemal A. Cancer statistics. CA: A Cancer Journal for Clinicians. 2019; 69: 7–34.
- [2] Holm J, Eriksson L, Ploner A, Eriksson M, Rantalainen M, Li J, *et al.* Assessment of Breast Cancer Risk Factors Reveals Subtype Heterogeneity. *Cancer Research*. 2017; 77: 3708–3717.
- [3] Haque W, Verma V, Hatch S, Suzanne Klimberg V, Brian Butler E, Teh BS. Response rates and pathologic complete response by breast cancer molecular subtype following neoadjuvant chemotherapy. *Breast Cancer Research and Treatment*. 2018; 170: 559–567.
- [4] Antunovic L, Gallivanone F, Sollini M, *et al.* [ $^{18}\text{F}$ ] FDG PET/CT features for the molecular characterization of primary breast tumors. *European Journal of Nuclear Medicine and Molecular Imaging*. 2017; 44: 1945–1954.
- [5] Agersborg S, Mixon C, Nguyen T, Aithal S, Sudarsanam S, Blocker F, *et al.* Immunohistochemistry and alternative FISH testing in breast cancer with her2 equivocal amplification. *Breast Cancer Research and Treatment*. 2018; 170: 321–328.
- [6] Gosselin K, Durand A, Marsolier J, Poitou A, Marangoni E, Nemati F, *et al.* High-throughput single-cell ChIP-seq identifies heterogeneity of chromatin states in breast cancer. *Nature Genetics*. 2019; 51: 1060–1066.
- [7] Cho N. Molecular subtypes and imaging phenotypes of breast cancer. *Ultrasonography*. 2016; 35: 281–288.
- [8] Guo W, Hao B, Luo N, Ruan D, Guo X, Chen H, *et al.* Early re-staging and molecular subtype shift surveillance of locally recurrent or metastatic breast cancer: a new PET/CT integrated precise algorithm. *Cancer Letters*. 2018; 418: 221–229.
- [9] Leithner D, Mayerhoefer ME, Martinez DF, *et al.* Non-Invasive Assessment of Breast Cancer Molecular Subtypes with Multiparametric Magnetic Resonance Imaging Radiomics. *Journal of Clinical Medicine*. 2020; 9: 1853.
- [10] Leithner D, Horvat JV, Marino MA, *et al.* Radiomic signatures with contrast-enhanced magnetic resonance imaging for the assessment of breast cancer receptor status and molecular subtypes: initial results. *Breast Cancer Research*. 2019; 21: 106.

- [11] Paydary K, Seraj SM, Zadeh MZ, Emamzadehfard S, Shamchi SP, Gholami S, *et al.* The Evolving Role of FDG-PET/CT in the Diagnosis, Staging, and Treatment of Breast Cancer. *Molecular Imaging and Biology*. 2019; 21: 1–10.
- [12] Lemarignier C, Martineau A, Teixeira L, Vercellino L, Espié M, Merlet P, *et al.* Correlation between tumour characteristics, SUV measurements, metabolic tumour volume, TLG and textural features assessed with 18F-FDG PET in a large cohort of oestrogen receptor-positive breast cancer patients. *European Journal of Nuclear Medicine and Molecular Imaging*. 2017; 44: 1145–1154.
- [13] Koolen BB, Vrancken Peeters MJTFD, Wesseling J, Lips EH, Vogel WV, Aukema TS, *et al.* Association of primary tumour FDG uptake with clinical, histopathological and molecular characteristics in breast cancer patients scheduled for neoadjuvant chemotherapy. *European Journal of Nuclear Medicine and Molecular Imaging*. 2012; 39: 1830–1838.
- [14] Kitajima K, Fukushima K, Miyoshi Y, *et al.* Association between <sup>18</sup>F-FDG uptake and molecular subtype of breast cancer. *European Journal of Nuclear Medicine and Molecular Imaging*. 2015; 42: 1371–1377.
- [15] Zhang J, Jia Z, Zhou M, Ragaz J, Zhang Y, Wang B, *et al.* The SUVmax for 18F-FDG Correlates with Molecular Subtype and Survival of Previously Untreated Metastatic Breast Cancer. *Clinical Nuclear Medicine*. 2013; 38: 256–262.
- [16] Sollini M, Cozzi L, Ninatti G, *et al.* PET/CT radiomics in breast cancer: Mind the step. *Methods*. 2021; 188: 122–132.
- [17] Ma W, Zhao Y, Ji Y, Guo X, Jian X, Liu P, *et al.* Breast Cancer Molecular Subtype Prediction by Mammographic Radiomic Features. *Academic Radiology*. 2018; 26: 196–201.
- [18] Sutton EJ, Oh JH, Dashevsky BZ, Veeraraghavan H, Apte AP, Thakur SB, *et al.* Breast cancer subtype intertumor heterogeneity: MRI-based features predict results of a genomic assay. *Journal of Magnetic Resonance Imaging*. 2015; 42: 1398–1406.
- [19] Sutton EJ, Dashevsky BZ, Oh JH, Veeraraghavan H, Apte AP, Thakur SB, *et al.* Breast cancer molecular subtype classifier that incorporates MRI features. *Journal of Magnetic Resonance Imaging*. 2016; 44: 122–129.
- [20] Chang R, Chen H, Chang Y, Huang C, Chen J, Lo C. Quantification of breast tumor heterogeneity for ER status, her2 status, and TN molecular subtype evaluation on DCE-MRI. *Magnetic Resonance Imaging*. 2016; 34: 809–819.
- [21] Yang Z, Sun Y, Xu X, Zhang Y, Zhang J, Xue J, *et al.* The Assessment of Estrogen Receptor Status and its Intratumoral Heterogeneity in Patients with Breast Cancer by Using 18F-Fluoroestradiol PET/CT. *Clinical Nuclear Medicine*. 2017; 42: 421–427.
- [22] Moscoso A, Ruibal Á, Domínguez-Prado I, Fernández-Ferreiro A, Herranz M, Albaina L, *et al.* Texture analysis of high-resolution dedicated breast 18 F-FDG PET images correlates with immunohistochemical factors and subtype of breast cancer. *European Journal of Nuclear Medicine and Molecular Imaging*. 2018; 45: 196–206.
- [23] Huang F, Shi Q, Li Y, Xu L, Xu C, Chen F, *et al.* Her2/EGFR-AKT Signaling Switches TGF $\beta$  from Inhibiting Cell Proliferation to Promoting Cell Migration in Breast Cancer. *Cancer Research*. 2018; 78: 6073–6085.
- [24] von Minckwitz G, Huang C, Mano MS, Loibl S, Mamounas EP, Untch M, *et al.* Trastuzumab Emtansine for Residual Invasive her2-Positive Breast Cancer. *The New England Journal of Medicine*. 2019; 380: 617–628.
- [25] Pesapane F, Rotili A, Agazzi GM, *et al.* Recent Radiomics Advancements in Breast Cancer: Lessons and Pitfalls for the Next Future. *Current Oncology*. 2021; 28: 2351–2372.
- [26] Nardone V, Boldrini L, Grassi R, *et al.* Radiomics in the Setting of Neoadjuvant Radiotherapy: A New Approach for Tailored Treatment. *Cancers*. 2021; 13: 3590.
- [27] Yan M, Wang W. Radiomic Analysis of CT Predicts Tumor Response in Human Lung Cancer with Radiotherapy. *Journal of Digital Imaging*. 2020; 33: 1401–1403.
- [28] Beukinga RJ, Wang D, Karrenbeld A, *et al.* Addition of HER2 and CD44 to <sup>18</sup>F-FDG PET-based clinico-radiomic models enhances prediction of neoadjuvant chemoradiotherapy response in esophageal cancer. *European Radiology*. 2021; 31: 3306–3314.
- [29] Fionda B, Boldrini L, D’Aviero A, Lancellotta V, Gambacorta M, Kovács G, *et al.* Artificial intelligence (AI) and interventional radiotherapy (brachytherapy): state of art and future perspectives. *Journal of Contemporary Brachytherapy*. 2020; 12: 497–500.
- [30] Zubor P, Kubatka P, Dankova Z, Gondova A, Kajo K, Hatok J, *et al.* MiRNA in a multiomic context for diagnosis, treatment monitoring and personalized management of metastatic breast cancer. *Future Oncology*. 2018; 14: 1847–186

**Supplementary material:** Supplementary material associated with this article can be found, in the online version, at <https://www.fbscience.com/Landmark/articles/10.52586/4960>.

**Abbreviations:** AUC, area under the curve; BC, breast cancer; <sup>18</sup>F-FDG PET/CT, <sup>18</sup>F-Fluorodeoxyglucose positron emission tomography/computed tomography; ER, estrogen receptor; FISH, fluorescence in situ hybridization; HER2, human epidermal growth factor receptor 2; IHC, immunohistochemistry; LASSO, least absolute shrinkage and selection operator; MTV, metabolic tumor volume; PR, progesterone receptor; ROC, receiver operating curve; SUV, standardized uptake value; TLG, total lesion glycolysis; TN, non-triple.

**Keywords:** Breast cancer; Radiomics; Molecular subtype classification; Positron emission tomography/computed tomography (<sup>18</sup>F-FDG PET/CT)

**Send correspondence to:**

Xiaofeng Li, Department of Molecular Imaging and Nuclear Medicine, Tianjin Medical University Cancer Institute and Hospital, National Clinical Research Center for Cancer, Key Laboratory of Cancer Prevention and Therapy, Tianjin’s Clinical Research Center for Cancer, 300060 Tianjin, China, E-mail: [xli03@tmu.edu.cn](mailto:xli03@tmu.edu.cn)

Wenjuan Ma, Department of Breast Imaging, Tianjin Medical University Cancer Institute and Hospital, National Clinical Research Center for Cancer, Key Laboratory of Cancer Prevention and Therapy, Tianjin’s Clinical Research Center for Cancer, 300060 Tianjin, China, E-mail: [mawenjuan@tmu.edu.cn](mailto:mawenjuan@tmu.edu.cn)

Wengui Xu, Department of Molecular Imaging and Nuclear Medicine, Tianjin Medical University Cancer Institute and Hospital, National Clinical Research Center for Cancer, Key Laboratory of Cancer Prevention and Therapy, Tianjin’s Clinical Research Center for Cancer, 300060 Tianjin, China, E-mail: [w Xu06@tmu.edu.cn](mailto:w Xu06@tmu.edu.cn)

† These authors contributed equally.